

Analyses and Comparison of Solar Air Heater with Various Rib Roughness using Computational Fluid Dynamics (CFD)

K. Ravi Kumar^{1*}, Muralimohan Cheepu², B. Srinivas¹, D. Venkateswarlu³,
G. Pramod Kumar¹, Apireddi Shiva⁴

¹Department of Mechanical Engineering, MVGR College of Engineering,
Andhra Pradesh 535005, India

²Department of Mechatronics Engineering, Kyungsung University, Busan 48434,
Republic of Korea

³Department of Mechanical Engineering, Marri Laxman Reddy Institute of
Technology and Management, Telangana 500043, India

⁴Department of Mechanical Engineering, Satya Institute of Technology and
Management, Andhra Pradesh 535002, India

*Corresponding author E-mail: kottalaravikumar15@gmail.com

Abstract. In solar air heater, artificial roughness on absorber plate become prominent technique to improving heat transfer rate of air flowing passage as a result of laminar sublayer. The selection of rib geometries plays important role on friction characteristics and heat transfer rate. Many researchers studying the roughness shapes over the years to investigate the effect of geometries on the performance of friction factor and heat transfer of the solar air heater. The present study made an attempt to develop the different rib shapes utilised for creating artificial rib roughness and its comparison to investigate higher performance of the geometries. The use of computational fluid dynamics software resulted in correlation of friction factor and heat transfer rate. The simulations studies were performed on 2D computational fluid dynamics model and analysed to identify the most effective parameters of relative roughness of the height, width and pitch on major considerations of friction factor and heat transfer. The Reynolds number is varied in a range from 3000 to 20000, in the current study and modelling has conducted on heat transfer and turbulence phenomena by using Reynolds number. The modelling results showed the formation of strong vortex in the main stream flow due to the right angle triangle roughness over the square, rectangle, improved rectangle and equilateral triangle geometries enhanced the heat transfer extension in the solar air heater. The simulation of the turbulence kinetic energy of the geometry suggests the local turbulence kinetic energy has been influenced strongly by the alignments of the right angle triangle.

1. Introduction

Now a days, the use of solar energy demands for various applications due to the problems of regular energy sources and many countries showing interest towards using of renewable energy. Solar energy is most efficient and tremendously freely available from the source of atmosphere and its need to absorb from the solar radiation. In past decades, many technologies developed to absorb the solar radiations to renovate it interested in solar energy for various solicitations. The ordinary solar absorber plates were showed low thermal efficiency and its need to improve by using artificial coatings to improve the roughness over the absorber plates in solar air heaters. The emitted solar radiations from the solar air



heaters are trapped using flat glass sheets and the radiations are contributes in heating of air which is flowing over the plates [1]. The solar heaters found to be easy to manufacture and cost reduction for the usage of rectangular cross sectional channels. There are many factors need to consider for the manufacturing of solar air heaters, which is become one of the main considerations of Reynolds number. In general, Reynolds number values are in 2000 to 16000 used in solar air heaters to maintain the turbulent nature of fluid flow [2]. The advancing technologies, replacing the regular solar heater absorber plates with artificial roughness to enhance its performance. The newly developed roughness phenomena artificially is typically avail for enlightening heat transfer rates in the channel which can led to change the flow pattern and resulted in breaking of laminar sublayer. However, it has some drawbacks that can aid to increases the friction factor and thus burden on the input power [3, 4]. The use of roughness in artificially on intense observed plate external plate is the efficient inactive technique for the enhancing heat in the absorber plate and transferring to its other side. Hence, the improvement in transferring rate of heat resulted in an inexorably excessive descent in pressure loss for the flow of the air or fluid. It is very important to minimize the friction losses that can be controlled by creating the turbulence in the region which is closed to the duct surface of laminar sublayer [4]. The air heaters used in solar energy comprises the physics of flow of the medium and flow of the heat and these two flows are expected with its performance of fluid pressure force, thermal and the combinations of both thermal and hydraulic efficiencies. Therefore the concert of thermal accompanies assessing the coefficient for the heat transfer and can be renovating it into thermal efficiency and Nusselt's number which is non-dimensional. In addition, solar air heaters thermal performance can be prophesied with advanced mathematical equations of Hottel-Whillier-Bliss which are defined through Duf-fie and Beckman [5]. The developed heaters for solar energy using applying of roughness imitation techniques are produced as the very thin wires of various sizes, contours and different directions on the stored device bottom side, which is amongst the most efficient technique for valued strategy enhances that the anticipated to progress the thermo-hydraulic concert [6]. The recent literature studies reported that the various experimental works extensively performed for enactment valuation of exaggeratedly roughed device. The manufacturing and application of these developed heaters may be originated in research reports of various researchers [7-23]. The previous literature reports revealed that very few studies have been conducted on computational fluid dynamics approach for assessing the enactment of artificially roughened of developed devices. The excellent outcome from simulation results gains the importance and rapid growth of powerful computer resources and development of computational fluid dynamics software packages which can solve the industrial problems efficiently. It is found that computational fluid dynamics has already recognized as a valid simulation tool for fluid flow and structure flow studies [3,24]. It is well known that the computational simulation of flow structure computed by various mathematical equations solving and its solutions given the output to govern the flow dynamics. In simulation, the results are the complete description of the three-dimensional flow in the entire results flow domain of the pressure distribution, velocity flow and temperature variations with density and other related physical properties in values and units. In simulation, the results are the complete description of the three-dimensional flow in the entire results flow domain of the pressure distribution, velocity flow and temperature variations with density and other related physical properties in values and units.

In most recent studies of the rib roughness in arc shape [25], reported the conventional solar air heaters performance using a CFD based simulation studies. To analyze the nature of the flow Ansys Fluent simulation tool and RNG $k-\varepsilon$ turbulence model were used and output of the results satisfy the experimental results. The study clearly indicated the effect of shape of the rib roughness and Reynolds number flow on the improvements of the several parameters reported. The simulation studies advances of 3D CFD were selected for metallic shingle artificial rib roughened device with computational fluid dynamics software FLUENT [26]. This model has been developed for various rib geometry shapes conditions and the model output also validated experimentally [24]. Many studies suggested different rib geometries and various parameters, but comparatively the standard design is not yet confirmed. In the present study, different rib geometries for developed devices with reproducing plates with roughness were selected for finding the variants in output efficiency of the flows to evaluate the hotness and its

transmission and hot air friction in a developed device using CFD simulation software. The comparison of the five different geometries simulation results are studied on improvement of the effectiveness and efficiency of solar air heaters.

2. Modeling of Geometry

In the present study, five different rib geometries are designed such as square rib, rectangle, equilateral triangle, improved equilateral triangle and right angle triangle. The schematic representation of the various rib geometries are illustrated in figure 1. The geometry outlines with ribs was produced in x-y plane with suitable proportions are given in table 1 (in mm) and at that point exterior parts was made from the fill option for 2-dimensional geometry and volume was generated from the extrude option for 3-dimensional geometry. The surface area of the different shapes of ribs was made equal while constructing the remaining geometries. The previous studies proposed that an appropriate 2D model is capable to provide the output of the simulation effectively the characteristics of forced convection and efficiency of turbulent flow were the solar air heater of artificially roughened having a rib shape of circular shape on the absorber plate. Due to this, there is no need of using such a complicated 3D models to analyse the simulation results [26]. The computational domain of 2D view has been selected for this study the purpose of reducing the computational time. The model was divided into three sections such as inlet, outlet and test section to evaluate the results easily using an ASHRAE standard method [27]. The meshing domain work was conducted on ANSYS software which is commercially available for generating the meshing in software. The final form of geometry which is created in CREO 2.0 was imported in ANSYS meshing. The prerequisite amount of separations and the type of “bias” were allotted to each and every edge. With the intention of to attain regular shape of rectangular one is the mesh cells with the best orthogonal excellence, and the facing option of the mapped was initiated. At the end of the modelling study the required mesh was engendered by providing the prerequisite tools buttons (see figure 2). The generated mesh was very fine in size and it was accomplished adjacent to the walls with the purpose of solving the apprehensive governing differential equations precisely in the form of linear flow so as to the laminar sub-layers by the side of the meshed regions. It is observed that the size of the generated mesh amplified in the direction of the centre region, as shown in figure 2. The grid size found to be constant for the size of length in entry and leaving segments of the surfaces of the duct. Also the results observed to be was confirmed the determined characteristic ratio of every grid at

Table 1 Geometrical parameters of different shapes of the rib

Geometrical parameters	Shape of the ribs				
	Square	Rectangle	Equilateral triangle	Modified triangle	Right angle triangle
Height of duct (H) (mm)	20	20	20	20	20
Height of rib (e) (mm)	3	2.5	3.89	2.34	4.5
Ratio in P/e	10	10	10	10	10
Length of test section (mm)	280	280	280	280	280
Outlet length (mm)	115	115	115	115	115
Width of duct (mm)	100	100	100	100	100
Inlet length (mm)	245	245	245	245	245

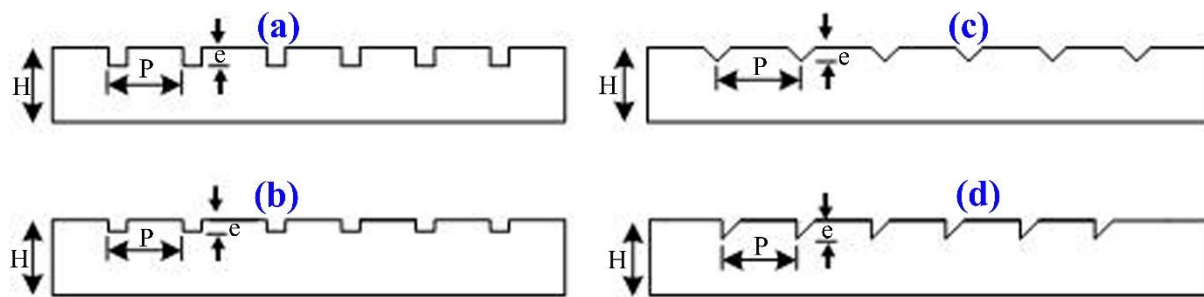


Figure 1 The geometries of the various designs of schematic representation (a) square, (b) rectangle, (c) equilateral triangle and (d) right angle triangle.

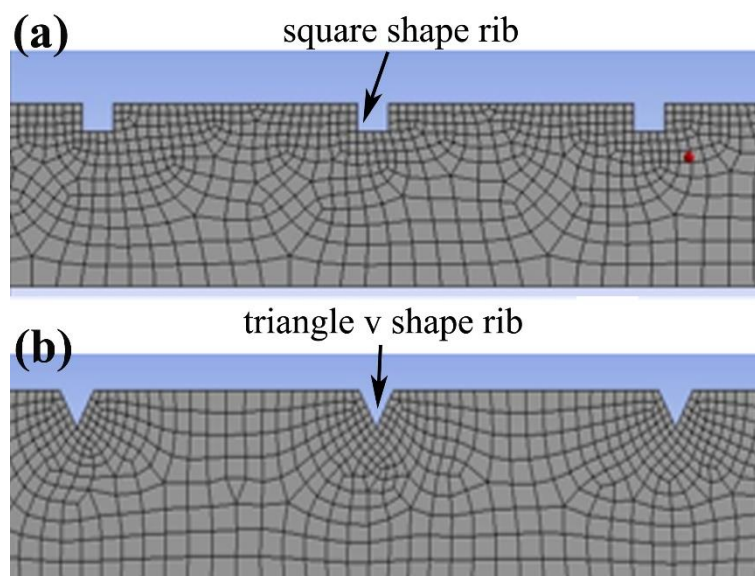


Figure 2 The developed design of meshing domains of the (a) square and (b) equilateral triangle shape rib roughness.

anyone was did not exceed 10. The mesh was created with acceptable values of orthogonal quality near to one and skewness factor near to less than 0.25. The generated meshing parameters and corresponding nodes information is provided in table 2, also the orthogonal quality and skewness are given.

The solver analysis parameters were selected to run the solution using CFD software after the successful completion of meshing domain. The continuum was chosen as fluid and the properties of water were assigned to it. To run the simulation, the analogous form of simulation tool FLUENT concurrently can calculates the equations for flow patterns by various processors/computers. However, the running software can be able to repeatedly separate the partition of the grid into different areas to allocate the computational work between accessible amounts of processors.

The selection of boundary conditions are a crucial for attaining accurate results in a CFD problem, are given in table 3. The inlet and outlet sections are defined as velocity inlet and pressure outlet respectively with a velocity corresponding to Reynolds number 3×10^3 to 18×10^3 at the inlet and static pressure 0 atm at the outlet. After the testing of the ribs, the separated sections comes the heated surface. It is divided that, top face is the wall with the selection of properties of wooden block. The boundary conditions are chosen from previous works which has given satisfactory results on similar simulations. [4]. The numerical model for fluid flow and heat transfer using an newly developed solar air heater with artificially roughened is should be followed the given expectations (a) fluid flow and heat transfer are in steady state (b) a completely developed flow of hydraulically and thermally (both should be in same steady state conditions), (c) duct wall thermal conductivity, roughness material and absorber plate all

are self-governing of temperature (d) absorber plate, the duct wall and roughness material are standardised and isotropic. The remaining all other walls are set adiabatic and the ambient temperature of air is set at 300 K for all iterations. The numerical model was used to investigate the 2D fluid flow phenomenon and heat transfer rates of solar air heater of techniques. Furthermore, advanced software package tools of 2D CFD model used for simulation for analysing newly developed device with an artificially roughened solar air heater through the viable CFD simulation tool in ANSYS FLUENT to resolve the conservation equations for the required parameters of momentum, mass and energy [28]. The solution domains usually consists of inlet, outlet and wall type of boundaries. The constant flux was given for the entire length of the ribs for all conditions. In the solution domain, the governing equations for the steady state flow are resolved by using software and the scrutiny is constructed on finite model volume approach.

Table 2 The selected meshing and nodes of the different geometries of the rib roughness

Meshing parameters	Shape of the rib				
	Square	Rectangle	Equilateral triangle	Modified triangle	Right angle triangle
Nodes	278558	384636	239283	467836	208171
Elements	246300	351232	210700	448016	183920
Orthogonal quality	0.9837	0.983	0.9835	0.939	0.9741
Skewness	0.1311	0.1316	0.1153	0.204	0.1611

Table 3 The boundary conditions used for the simulation studies

S.no	Boundary	Type	Properties
1	Inlet	Velocity inlet	0.5 m/s
2	Outlet	Pressure outlet	Gauge pressure=0
3	Absorber plate	Heat flux	1100 w/m ² k
4	Wall	Insulated	Insulated

3. Results and Discussions

The analysis of the modelling works which are computational basis are solved by using equations of Navier-Stokes, these are the main source of problem solving and are mathematically represented by finite volume method (FEM). In CFD model, the results accuracy is highly affected and depending on the turbulence model. Generally, the solar air heaters are designed using swirl or vortex flow to advance the mass and temperature distribution or heat transmission performance of the solar products with the allowance of minimal loss of pressure. To use the artificial roughness, the outline of the rudimentary wing is categorised as rectangular, triangular, and other delta categories are used to produce the vortex flow. Whereas, to achieve the turbulent field synergy the suitable form of the optimal conditions of the various flow patterns are needed. In the model a combination of heat transfer added to the solid baffles. The designed solid baffles of square and equilateral triangle roughness are most efficient and commonly preferred heat transfer techniques. The CFD simulation analysis of 2-dimensional duct of solar air heater was conducted to analyse the influence of pitch of the roughness ration of (P/e), comparative height of

the roughness and Reynolds number. Also, flow friction characteristics were used for the artificial roughness in the form of square and equilateral triangle rib roughness. The output of the results obtained from the simulations was smooth duct with almost similar flow and thermal boundary conditions. It is also observed that the increase in Reynolds number the outlet temperature gradually decreasing irrespective of the P/e ratios. The ratio of P/e values have significant effect on thermal behaviour and heat transfer flow to the solar heaters. The P/e ratio values are achieved similar condition when the minimum and maximum values are below 8 and above 13.33, respectively. The temperature distribution almost similar trend followed for these two conditions. Whereas, when the P/e ratio have optimum level the results are entirely different and achieved the maximum temperature distribution trend at P/e ratio of 10 %. The results obtained for P/e ratio at 10 is unlikely of P/e values of 8 and 13.3 and are always higher than the minimum and maximum values of Reynolds number can be at any point. The plot of the typical values in Reynolds number for various data points of the pitch of relative roughness and for constant values of the height of relative roughness (ratio of P/e), has been illustrated in figure 3. The aggregate Reynolds number surges in regard to ordinary surface of the duct by inserting the rib in square shape on the bottom of the plate of the duct of solar air heater. Furthermore, noticed the rise in Reynolds number resulting of reduction of laminar sub-layer thickness. The outlet temperature was suddenly dropped from 325 K to 310 K with the raise in Reynolds number from 3000 to 6000, respectively. Therefore, the generation of turbulence on the local wall owed to movement departure and return to attaching among them which can enrich the heat transfer rate. The development of artificial roughness rib techniques aid to generate vortices and hence influence of flow mixing, which is subsidize to avoid or remove the produced heat as of the absorber plate temperature surfaces. It is the fact that escalation in Reynolds number resulted in increases the turbulent dissipation and kinetic energy; those are in initiating for enhancing of Nusselt number and turbulent intensity. The simulated CFD results exhibits in contour graphs which is easy to understand the heat transfer phenomena and turbulent kinetic energy efficiently. These graphs are able to show the temperature, pressure and friction factor values where the

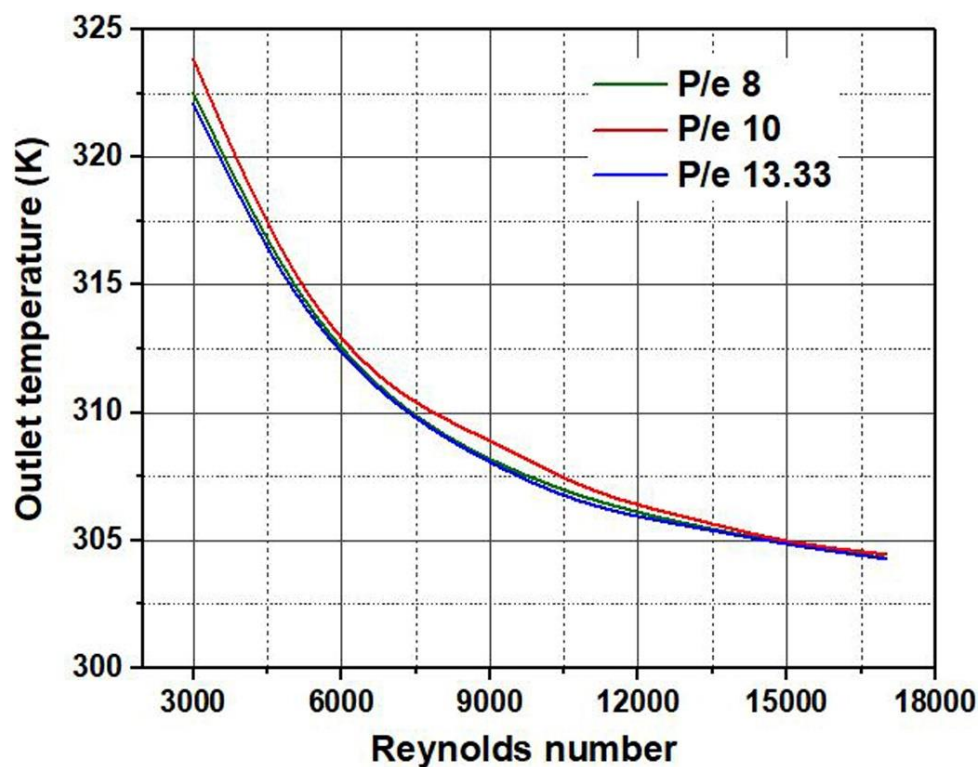


Figure 3 The change in temperature with the relationship between P/e ratio and Reynolds number.

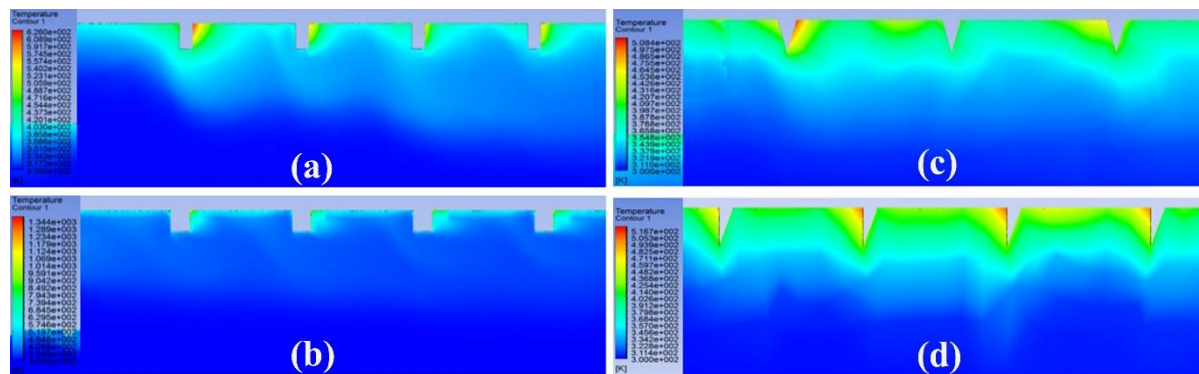


Figure 4 Temperature distribution of 2D square rib roughness (a) square, (b) rectangle, (c) equilateral triangle and (d) right angle triangle

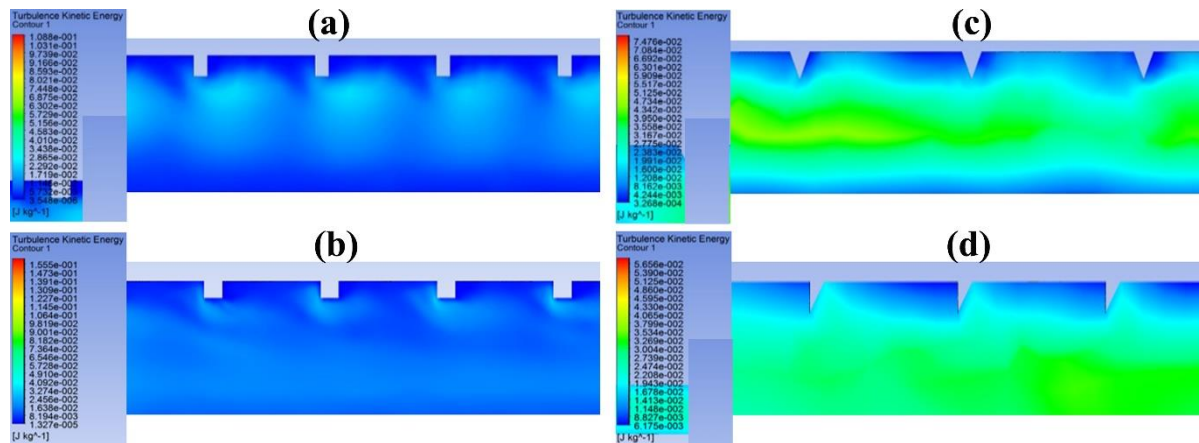


Figure 5 The obtained results of turbulent kinetic energy at $Re = 10,000$ with $P/e = 10$ at a height of the ribs of the relative roughness of (a) square, (b) rectangle, (c) equilateral triangle and (d) right angle triangle

maximum and minimum values distributed and its intensity clearly. The variation in intensity of the colour over the ribs roughness thickness volume. The corner of the square shaped rib roughness exhibits highest intensity of the temperature values and its intensity gradually decreasing towards underside of the ribs.

The maximum volume fraction of temperature distribution is higher for equilateral triangle shaped type roughness ribs over the square type roughness ribs. The intensity pattern graphs of temperature distribution of the various values of height of the relative roughness at a constant Reynolds number 10,000 with the ratio of P/e is 10, is revealed in figure 4. The maximum value of temperature is obtained near the top side of the wall and reducing towards bottom side of the rib. However the heat transfer occurrences were implicit effectively by the CFD results of form plot of the turbulent kinetic energy. For the right angel triangle design, the maximum temperature flow occurred at vertical wall where the sharp corner exposed at the top of the surface. Whereas, in equilateral triangle, the maximum temperature exhibits at inclination wall. The major difference in temperature flow has been developed with the minor changes in the modifications. Figure 5 exhibits the simulation results of form plot of the kinetic energy of turbulent flow for changes in height of the roughness values and Reynolds number of 10,000 at a virtual roughness to pitch ratio (P/e) numbers in 10. The simulation clearly illustrates the significant variation in the turbulent kinetic energy for the square and equilateral triangle shaped roughness heights. Among the four different geometries of rib roughness, right angle triangle shows the better performance. The highest intensity of the turbulence is shown in the contour graphs at bottom of

the thickness, where the less effect on the friction factor. In addition, it is gradually reduced to bottom of the roughness height. The highest value of 6.95 J/kg and minimum value is 2.11 J/kg of turbulent kinetic energy was recorded. Whereas, equilateral triangle shaped roughness heights shows the highest value of 7.47×10^{-2} J/kg and minimum value of 3.26×10^{-2} J/kg has been obtained. Unlike square shaped roughness height, triangle shaped contour plot illustrates the very less amount of intensity factor of turbulent kinetic energy. It is worth to mention that the recorded values are not all dangers to operating conditions and surely the efficiency is much higher compared to the square shaped roughness height on the solar air heater ribs. In case of square and equilateral ribs of the contour plots shows the agglomeration of turbulence kinetic energy just below the top surface, it is not able to distribute thought the thickness of the ribs. Whereas, rectangle shaped ribs are shows the flow streams from top surface to mid-section in the forward direction, these can results in better performance than the square and equilateral rib roughness. The design of right angle triangle is quite interesting and its contour plot illustrates the very less intensity of the turbulence kinetic energy streams formation in the any thickness point. It is able to distribute the temperature and turbulence factors easily to the bottom side and improve the performance. Among the all of the rib geometries, right angle triangle designs have the very lowest values of maximum turbulence kinetic energy of 5.62×10^{-2} J/kg. The minimum value of 6.1×10^{-3} J/kg recorded at the top of the inclination wall. The maximum and minimum values of turbulence kinetic energy of square, equilateral, improved equilateral, rectangle ribs are higher than the right angle triangle rib geometry. It has good flow streams and always showing the good performance over the others and also the friction factor is minimal.

Moreover, the highest values and intensity of turbulent kinetic energy created in mid-section of the triangle shaped roughness heights. The upper and lower parts to the mid-section are contained the similar view of the intensity. The appearance of this results led to more efficient results in the heat transfer point of view. However, in all the conditions it is detected that the turbulent kinetic energy lowers the increasing of distance from the wall. As illustrated in figure 3, Reynolds number increasing trend showing the resulting of roughness elements start to produce above the laminar sublayer. It is also noticed that as the Reynolds number increases, laminar sublayer gradually decreases. As perceived in figure 5b, the highest intensity of turbulent kinetic energy at mid-section, the heat removal also influenced by the local contribution (thickness) of the by vortices instigating from the roughness [3,29],

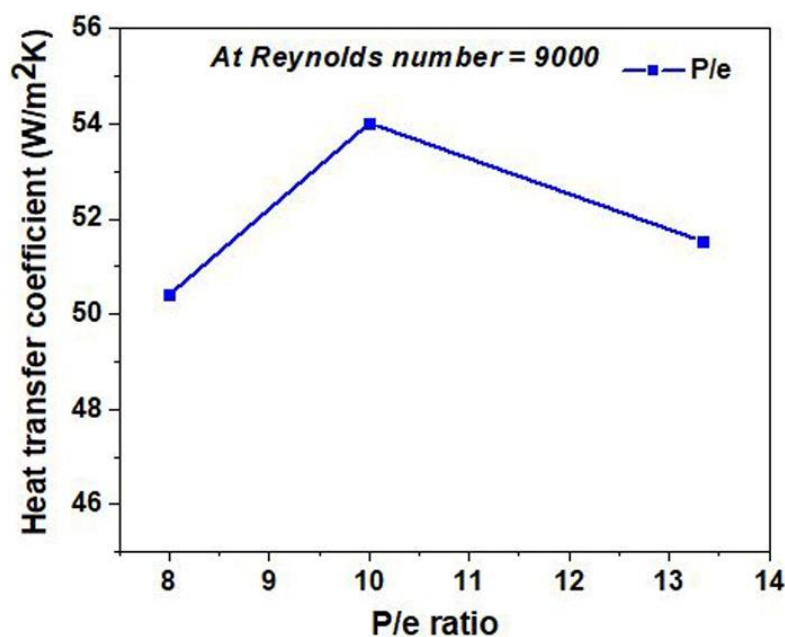


Figure 6 The correlation between the heat transfer rate and different P/e ratios at constant Reynolds number of 9000.

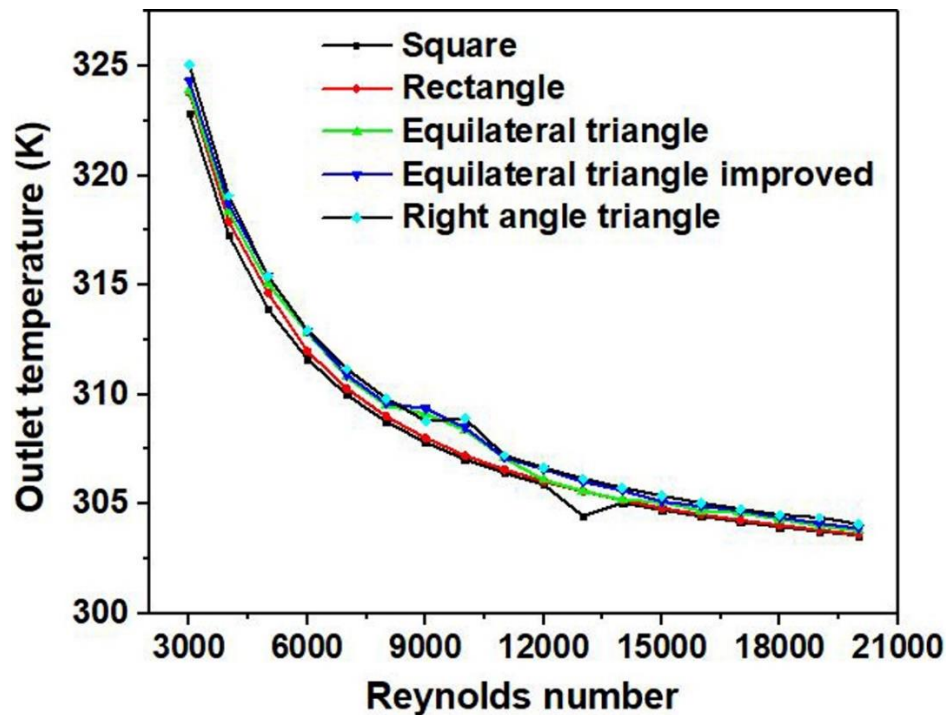


Figure 7 Variation of outlet temperature along with different rib roughness and Reynolds number of different rib roughness.

Table 4 The output of the simulation results of different roughness shaped used

Parameter	Square rib	Rectangle rib	Equilateral triangle rib	Equilateral triangle with improved roughness rib	Right angle triangle rib
Heat input (W/m ²)	1100	1100	1100	1100	1100
Temperature (inlet) (K)	300	300	300	300	300
Temperature (outlet) (K)	322.84	323.78	323.89	324.31	325.05
% increase in outlet temperature	7.61	7.92	7.96	8.1	8.35
Improvement in heat transfer coefficient	3.21	3.31	3.35	3.42	3.47

and thus cause to rising in heat transfer rate of artificially roughness surface associated with ordinary rib surface. From the results, it is also important to determine the velocity of the entering and outlet flow velocity with the intention of understand the result of roughness shape and height. As the roughened duct length of the device considers, it is expecting to determining of the flow velocity entering from the inlet is lesser as compared to leaving from outlet of the duct. It is owing to the velocity flow acceleration in the form of stream-wise direction [3,15]. It is also observed that the instantaneous flow velocity contours of the equilateral triangular roughness ribs is regular and smooth and concentrated path followed, whereas, in square shaped roughness ribs velocity contours illustrates the irregular way, due to the wide path of the square shaped roughness and less concentration vertices can be expecting that it is the nature of the turbulence for square sectioned transverse ribs. The correlation between the P/e ratio

and heat transfer coefficient at Reynolds number 9000 are shown in figure 6. The highest heat transfer coefficient obtained for P/e ratio of 10, and its gradually reduced at 13.33 ratio of P/e value. Figure 7 illustrates the outlet temperature of the five types of artificial roughened ribs with respect to Reynolds number. The improved equilateral triangle design shows quite better results than the equilateral triangle rib roughness. The outlet temperatures at all the conditions were lowering with the rise in Reynolds number. The equilateral triangle shaped roughened ribs quite higher than the square shaped ribs, it is because of the concentrated flow of velocity from the triangle groove. The friction factor values are changes between five types of shaped roughens ribs. In all the conditions it is found that the increase Reynolds number the led to decrease in friction factor. It is owing to the lowering of viscous sublayer with rises of Reynolds number as explained the phenomena from the figure 3. The effect of artificial roughened solar heaters are clearly indicates the producing higher friction factor than the smooth surface of the solar heaters. The friction factor achieved very less value among the five types of designs that the right angle triangle geometry ribs. The change in friction factor also affected by the height of the roughness intended for a constant plot of relative roughness shape of the pitch size [30,31]. The friction factor values were observed at a 0.045 value of height of the relative roughness and Reynolds number is 3010. Simulations of the overall results for the square, rectangle, equilateral triangle, improved equilateral triangle and right angle triangle shaped roughened ribs are given in table 4. The outlet temperature of the right angle triangle dropped suddenly at Reynolds number of 13000, and which suggests that the right angle triangle shaped artificial roughened ribs higher performance than the all other geometries of the ribs.

4. Conclusions

In this study, 2D analyses have been performed to investigate the effect of square, rectangle, equilateral triangle, improved equilateral triangle and right angle triangle sectioned rib roughness on heat transfer performance on solar air heaters which are developed by artificially roughened for Reynolds number of 3000 to 20000. The outlet temperature gradually reduced Reynolds number above the 8000 because of formation of the area which is covered by low heat transfer with the influence of crosswise movement flow of the air flow towards bottom parts of the rib. This phenomena is clear and simulation results confirmed for the right angle triangle rib roughness. The ratio of P/e is 10 has the better results and the geometry of the rib sizes are recommended at this ratio. The ratio of roughness height and pitch has strong effect on the flow pattern and effectiveness of the artificially roughened device. Among the five types of geometries, the friction factor values for shaped in square ribs was found to be higher and followed by equilateral, rectangle and right angle triangle. The outlet temperature of the right angle triangle dropped suddenly at Reynolds number of 13000, and which suggests that the right angle triangle shaped artificial roughened ribs higher performance than the all other geometries of the ribs. The amount of the turbulence kinetic energy flow was in downstream direction compared to the other type of geometry of the rib roughness.

References

- [1] Hans V S, Saini R P and Saini J S 2009 Performance of artificially roughened solar air heaters - a review, *Renew. Sustain. Energy. Rev.* **13** (8) 1854-69.
- [2] Charters W W S 1971 Some aspects of flow duct design for solar-air heater applications *Solar. Energy.* **13** 283-88.
- [3] Varun, Saini R P and Singal S K 2007 A review on roughness geometry used in solar air heaters, *Solar. Energy.* **81** 1340-50.
- [4] Kumar R, Geol V and Kumar A 2017 A parametric study of the 2D model of solar air heater with elliptical rib roughness using CFD *J. Mech. Sci. Technol.* **31**(2) 959-64.
- [5] Duffie J A and Bekman W A 1980 Solar engineering of thermal processes 2nd ed. *New York Wiley.*
- [6] Hans V S, Saini R P and Saini J S 2009 Performance of artificially roughened solar air heaters-a review *Renew. Sustainable. Energy. Rev.* **13** 1854-69.

- [7] Chandra P R, Alexander C R, and Han J C 2003 Heat transfer and friction behaviors in rectangular channels with varying number of ribbed walls *Int. J. Heat. Mass. Transfer.* **46** 481-95.
- [8] Muralimohan C H, Haribabu S, Reddy Y H, Muthupandi V and Sivaprasad K 2015 Joining of AISI 1040 steel to 6082-T6 aluminium alloy by friction welding *J. Adv. Mech. Eng. Sci.* **1(1)** 57-64. <http://dx.doi.org/10.18831/james.in/2015011006>
- [9] Muralimohan C H, Muthupandi V and Sivaprasad K 2014 The influence of aluminium intermediate layer in dissimilar friction welds *Inter. J. Mater. Res.* **105** 350-57.
- [10] Cheepu M, Muthupandi V, Srinivas B and Sivaprasad K 2018 Development of a friction welded bimetallic joints between titanium and 304 austenitic stainless steel *Techno-Societal 2016, International Conference on Advanced Technologies for Societal Applications ICATSA 2016 ed Pawar P M, Ronge B P, Balasubramaniam R and Seshabhattachar S (Springer, Cham) Chapter 73* 709-17. https://doi.org/10.1007/978-3-319-53556-2_73
- [11] Bhushan B and Singh R 2010 A review on methodology of artificial roughness used in duct of solar air heaters *Energy.* **35** 202-12.
- [12] Cheepu M, Ashfaq M and Muthupandi V 2017 A new approach for using interlayer and analysis of the friction welding of titanium to stainless steel *Trans. Indian. Inst. Met.* **70** 2591-600. <https://doi.org/10.1007/s12666-017-1114-x>
- [13] Muralimohan C H, Ashfaq M, Ashiri R, Muthupandi V and Sivaprasad K 2016 Analysis and characterization of the role of Ni interlayer in the friction welding of titanium and 304 austenitic stainless steel *Metall. Mater. Trans. A.* **47** 347-59.
- [14] Cheepu M M, Muthupandi V and Loganathan S 2012 Friction welding of titanium to 304 stainless steel with electroplated nickel interlayer *Mater. Sci. Forum.* **710** 620-25.
- [15] Kumar A, Saini R P and Saini J S 2012 Heat and fluid flow characteristics of roughened solar air heater ducts-a review *Renew. Energy.* **47** 77-94.
- [16] Muralimohan C H, Haribabu S, Reddy Y H, Muthupandi V and Sivaprasad K 2014 Evaluation of microstructures and mechanical properties of dissimilar materials by friction welding *Procedia. Mater. Sci.* **5** 1107-13.
- [17] Muralimohan C H, Muthupandi V and Sivaprasad K 2014 Properties of friction welding titanium-stainless steel joints with a nickel interlayer *Procedia. Mater. Sci.* **5** 1120-29.
- [18] Muralimohan C H and Muthupandi V 2013 Friction welding of type 304 stainless steel to CP titanium using nickel interlayer *Adv. Mater. Res.* **794** 351-57.
- [19] Cheepu M, Muthupandi V and Che W S 2018 Improving mechanical properties of dissimilar material friction welds *Appl. Mech. Mater.* **877** 157-62. doi:10.4028/www.scientific.net/AMM.877.157
- [20] Venkateswarulu D, Cheepu M, Krishnaja D and Muthukumaran S 2018 Influence of water cooling and post-weld ageing on mechanical and microstructural properties of the friction-stir welded 6061 aluminium alloy joints *Appl. Mech. Mater.* **877** 163-76. doi:10.4028/www.scientific.net/AMM.877.163
- [21] Cheepu M, Haribabu S, Ramachandraiah T, Srinivas B, Venkateswarulu D, Karna S, Alapati S and Che W S 2018 Fabrication and analysis of accumulative roll bonding process between magnesium and aluminum multi-layers *Appl. Mech. Mater.* **877** 183-89. doi:10.4028/www.scientific.net/AMM.877.183
- [22] Devireddy K, Devuri V, Cheepu M and Kumar B K 2018 Analysis of the influence of friction stir processing on gas tungsten arc welding of 2024 aluminum alloy weld zone *Int. J. Mech. Prod. Eng. Res. Dev.* **8(1)** 243-52. DOI: 10.24247/ijmperdfeb201828
- [23] Cheepu M, Venkateswarlu D, Mahapatra M M and Che W S 2017 Influence of heat treatment conditions of Al-Cu aluminum alloy on mechanical properties of the friction stir welded joints *Korean Welding and Joining Society*, 11 264-264. <http://www.dbpia.co.kr/Journal/ArticleDetail/NODE07278590>

- [24] Karmare S V and Tikekar A N 2010 Analysis of fluid flow and heat transfer in a rib grit roughened surface solar air heater using CFD *Sol. Energy*. **84** 409-17.
- [25] Kumar S and Saini R P 2009 CFD based performance analysis of a solar air heater duct provided with artificial roughness *Renew. Energy*. **34** 1285-91.
- [26] Yadav A S and Bhagoria J L 2013 A CFD based heat transfer and fluid flow analysis of a solar air heater provided with circular transverse wire rib roughness on the absorber plate *Energy*. **55** 1127-42.
- [27] ASHRAE Standard 93 Method of testing to determine the thermal performance of solar collectors *American society of heating, refrigeration and air conditioning engineers* Atlanta **GA30329** 2003.
- [28] <http://www.ansys.com/academic/free-student-products>
- [29] Webb R L and Eckert E R G 1972 Application of rough surfaces to heat exchanger design *Int. J. Heat. Mass. Transfer*. **15** 1647-58.
- [30] Chandra P R, Alexander C R and Han J C 2003 Heat transfer and friction behaviors in rectangular channels with varying number of ribbed walls *Int. J. Heat. Mass. Transfer*. **46** 481-95.
- [31] Bharadwaj G, Kaushal M and Goel V 2013 Heat transfer and friction characteristics of an equilateral triangular solar air heater duct using inclined continuous ribs as roughness element on the absorber plate *Inter. J. Sustain. Energy*. **32(6)** 515-30.